International Journal of Pharmacy and Biological Sciences
ISSN: 2321-3272 (Print), ISSN: 2230-7605 (Online)
IJPBS | Volume 9 | Special Issue 2 | 2019 | 373-391
| Research Article | Biological Sciences |Open Access |MCI Approved|
|UGC Approved Journal|

A Comparative Study for The Adsorptive Removal of Toxic Heavy Metal Lead (II), Copper (II) Using Chitosan Oligosaccharide - Graft - Maleic Anhydride / Silk Fibroin Composite

P. Ajitha, M. Saranya, T. Gomathi and P. N. Sudha*
P.G and Research Department of chemistry, D.K.M. College for Women, Vellore, Tamil Nadu.

Received: 30 Jan 2019 / Accepted: 20 Feb 2019 / Published online: 01 Apr 2019
Corresponding Author Email: drparsu8@gmail.com

Abstract
The present work was aimed to prepare the novel chitosan oligosaccharide-graft-maleic anhydride/silk fibroin composite for the adsorptive removal of toxic heavy metal lead (II) and Copper (II). The results revealed that the grafted chitosan oligosaccharide copolymer was mixed homogeneous with silk fibroin through intermolecular hydrogen bonding The SEM micrographs revealed that surface morphology of COS is suitable for metal adsorption, while FTIR analysis confirmed presence of various active groups (O- H, C= O, C- O- C, C= C and amide II) which could interact with metal ions. The adsorption experiments were performed in batch system. Experimental data were fitted by pseudo – first order and pseudo – second order kinetic models as well as Langmuir and Freundlich isotherm models. Biosorption of the both metals follow pseudo second-order kinetic model. The best fitting adsorption model is Langmuir model and the maximum biosorption capacities. Batch adsorption studies was carried out to study the removal efficiency of the prepared composite by varying the parameters such as pH, contact time, adsorbent dose and initial metal ion concentration using the synthetic copper solution. From the results, it was concluded that the graft copolymer was found to be an efficient adsorbent.

Keywords
Grafting; Chitosan Oligosaccharide; Maleic anhydride; Silk Fibroin; Adsorption, Biosorption, Freundlich and Langmuir Isotherm.

*****

INTRODUCTION
Water is the most common, finite, precious and the widespread natural resource on earth essential for all living organisms (Yasmin Regina et al., 2015). At present, these toxic metals have polluted our atmosphere, our water, soil and food chain, and have been reported to be slightly toxic even at low concentration (Chehregani et al., 2004). Biopolymers are an important source of material with a high chemical versatility and with high potential to be used in a range of biomedical applications (Mano et al., 2004).

In recent years, many researchers focused on the water-soluble chitosan with lower molecular weight,

chitosan oligosaccharide (COS), to synthesize the chitosan oligosaccharide hydrophobic derivatives for the controlled release of hydrophobic antitumor drug (Zhang et al., 2006; Dong and Feng, 2006). Graft copolymerization of chitosan oligosaccharide is expected to be one of the most promising approaches to a wide variety of molecular designs leading to novel types of hybrid materials, which are composed of bio- and synthetic polymers (Vijayakumar Thakur and Manju Kumari Thakur, 2015). Ammonium cerium (IV) nitrate, is also called as ceric ammonium nitrate or "CAN", ammonium nitrato cerate (IV) and ammonium hexanitrato cerate (IV). It is an oxidizing agent widely used in organic synthesis. CAN can also be used as nitrating agent, initiator for radical polymerization reactions (Karen Deleersnyder et al., 2009). Maleic anhydride had been used for grafting of chitosan oligosaccharide. Due to the presence of highly reactive anhydride group in maleic anhydride they are generally used in grafting (Mirabedini et al., 2004).

The blending and grafting of synthetic polymers are the convenient methods to add new properties to the natural polymer with minimum loss of the initial properties of the substrate. Polyvinyl alcohol (PVA) is a synthetic hydrophilic polymer widely used as emulsificants, adhesives, in textile and paper industry applications and in the attainment of amphiphilic membranes for enzyme immobilization due to its excellent properties such as non-toxic, bio-compatible, biodegradable, good mechanical properties, tensile strength, good fibre and film forming ability and flexibility (Farrokh Sharifi et al., 2016).

The purpose of using polyvinyl alcohol in heavy metal removal is that the PVA has unpaired electrons while the heavy metals have valence shells and hence by the 18-electron rule the unpaired electrons of PVA will bond with the heavy metal ion valence shells resulting in the easy removal of heavy metal ions from water (Mohammad Al-Hwaiti et al., 2015).

Chitosan-g-maliec anhydride-g-ethylene di-methacrylate was prepared to remove chromium and copper from aqueous solution, and they were effectively removed (Gopal redii et al.,2017). Lavanya et al., (2017) prepared chitosan-g-maleic anhydride-g-methacrylic acid copolymer and removed lead (II) and copper (II) from aqueous solution. It was found that prepared adsorbent was suitable for the removal of heavy metals from wastewater.

Since work on grafted chitosan oligosaccharide are very few in the present research work grafted chitosan oligosaccharide was blended with polyvinyl alcohol and used for the removal of heavy metals Pb (II) and Cu(II) ions from wastewater.

Therefore, to modify the grafted chitosan oligosaccharide blended polyvinyl alcohol, it was further mixed with the biopolymer silk to form composites. Silk fibrion is a kind of natural fibrous polymer produced by domestic silk worms (*Bombyxmori)* and is made up of 18 kinds of amino acids, such as glycine, alanine, sericine and so on. It has many unique physicochemical properties and good biocompatibility that is especially attractive. In non-textile fields, in addition to being used as surgical sutures, it is used as food additives and in the cosmetic industry (Minoura et al., 1990). This prepared composite was used for the removal of heavy metals Pb (II) and Cu (II) ions from wastewater. The sorption mechanism was further studied using equilibrium adsorption isotherm and kinetic studies.

MATERIALS AND METHODS

Materials

The chitosan oligosaccharide was purchased from India Sea foods, Cochin, Kerala. Cocoons of *Bombyxmori* were obtained from the sericulture farm in Vaniyambadi, Vellore District. The chemicals namely the polyvinyl alcohol and maleic anhydride were purchased from Sigma Aldrich, India and Thomas Baker Chemicals Private Ltd, Mumbai respectively. The initiator, ceric ammonium nitrate (Ce $(NH_4)_2(NO_3)_6$) was purchased from Thomas Bakers chemicals and all the reagents used in the present research work were of analytical grade.

Preparation of silk

In order to remove the sericin, the *Bombyxmori* silk was boiled in 0.5% Wt. of Na_2CO_3 aqueous solution for 40 minutes, then rinsed three times successively in distilled water and soaked in distilled water overnight. The degummed silk was dried in an oven at 60°C for 7 hrs.

Preparation of chitosan oligosaccharide-g-maleic anhydride

About 5 g of chitosan oligosaccharide was dissolved in 30 mL of water and stirred well to form a homogeneous solution. 2.5 g of maleic anhydride monomer dissolved in 30 mL of water was then added

to the above prepared homogenous (COS) solution. In order to initiate the polymerization process in the above mixture, the initiator ceric ammonium nitrate (CAN) (0.5 g of CAN in 10 mL of 1 N HNO_3) was added and after all the addition was over, the above mixture was heated to 70°C and simultaneously the stirring of that mixture was performed for a period of approximately 30 min using a magnetic stirrer. After a time period of 30 minutes, the above solution was poured into excess sodium hydroxide (2N) solution to precipitate the graft copolymer. Finally, the obtained graft copolymer precipitated was washed several times in distilled water then filtered, dried and weighed.

Preparation of chitosan oligosaccharide-g-maleic anhydride/polyvinyl alcohol

About 1g of the above prepared chitosan oligosaccharide-g-maleic anhydride copolymer (COS-g-MAH) was dispersed in minimum amount of water. A required amount of polyvinyl alcohol (1.0 ml) dissolved in minimum amount of hot water was added to the above prepared COS-g-MA copolymer solution which was then kept under constant magnetic stirring for about half an hour and then finally poured into petri plates, allowed to dry for few hours, until dry. Same procedure has been repeated for various ratios such as (1:1) ;(1:2) ;(2:1).

Preparation of chitosan oligosaccharide-g-maleic anhydride/polyvinyl alcohol/ silk fibroin composite

About 1g of the above prepared chitosan oligosaccharide-g-maleic anhydride copolymer (COS-g-MAH) was dispersed in minimum amount of water. A required amount of polyvinyl alcohol (1.0 ml) dissolved in minimum amount of hot water was added to the above prepared COS-g-MA copolymer solution which was then kept under constant magnetic stirring for about half an hour. After this process was over, the required amount of silk fibroin (0.25g) chopped into fine pieces of around 0.1 cm was added onto the COS-g-MAH copolymer/PVA solution mixture followed by the effective blending process using the magnetic stirrer for a period of 30 minutes and then finally poured into petri plates, allowed to dry for few hours, until dry. Same procedure has been repeated for various ratios such as (1:1:0.25) ;(1:1:0.5) ;(1:1:1).

CHARACTERISATION

Fourier Transform Infra-Red Spectral Analysis

Measurements were performed with Thermo Nicolet AVATAR 330 spectrophotometer in 4000 – 400cm^{-1} wave length range using KBr pellet method.

Scanning Electron Microscopy

The surface morphology of the composites was observed with scanning electron microscopy to verify the compatibility of the polymers. For the analysis, the composites were cut into pieces of various sizes and wiped with a thin gold – palladium layer by a sputter coater unit (VG – microtech, UCK field, UK) and the cross section topography was analysed with Cambridge stereoscan 440 scanning electron microscope (SEM, Leica, Cambridge, UK).

RESULT AND DISCUSSION

Mechanism

The newly functionalized chitosan oligosaccharide-graft-maleic anhydride/polyvinylalcohol/silk fibroin (COS-g-MAH/PVA/SF) is regarded as a composite of different functiona lgroups that are expected to form various coordination complexes with metal ions. The functional groups responsible for binding with heavy metal ions are generally in the form of amine (-NH2) and hydroxyl (-OH). Based on the results obtained by various researchers (L.Xu, Y.A. Huang et al.,2015) the following mechanism was proposed for the formation of chitosan oligosaccharide-graft-maleic anhydride copolymer. In addition, the mechanism of formation of chitosan oligo saccharide graft maleican hydride/polyvinyl alcohol/sik fibroin composite and the binding of Pb (II) and Cu (II) ions onto chitosan oligosaccharide-graft-maleic anhydride/polyvinyl alcohol/silk fibroin composite was also represented in Figure-24.

FTIR Spectral Analysis

Figure 1: FTIR spectrum of pure COS

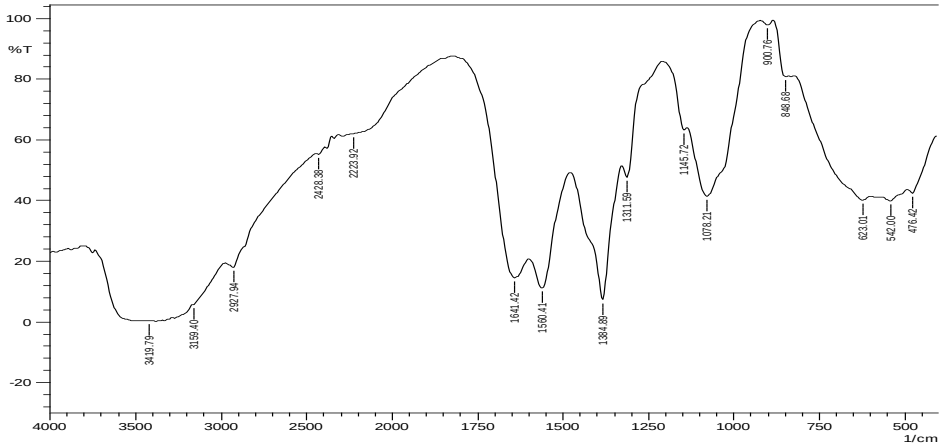

Figure 2: FT-IR spectrum of COS- g -Maleic anhydride copolymer

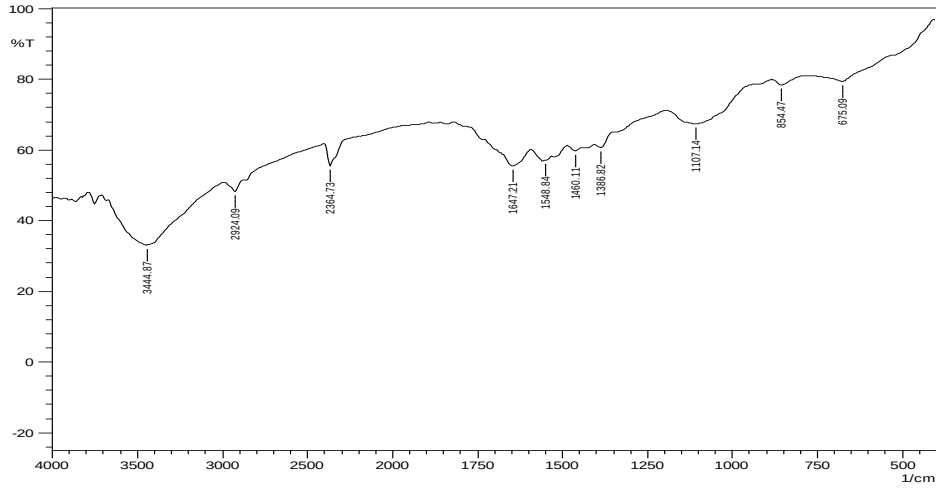

Figure 3: FTIR Spectrum of COS-G-MAH/PVA (1:1) blend

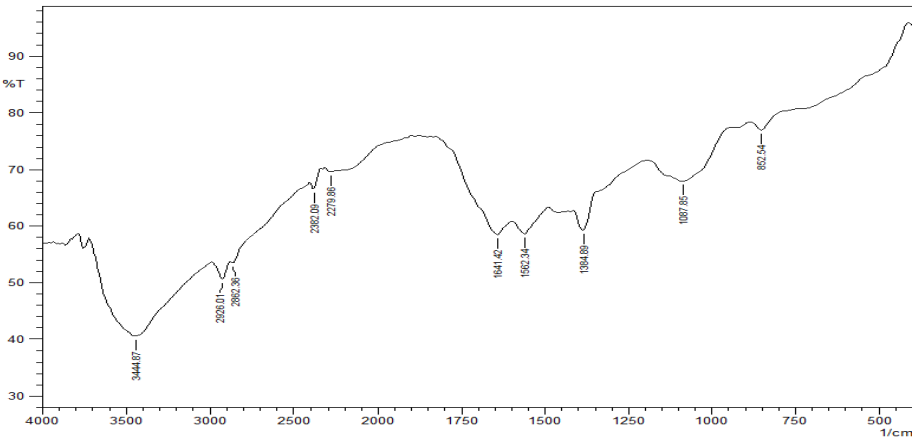

Figure-4: FTIR Spectrum of Chitosan oligosaccharide – g – maleic anhydride /Polyvinyl Alcohol/ Silk Fibroin (1:1:0.25) composite

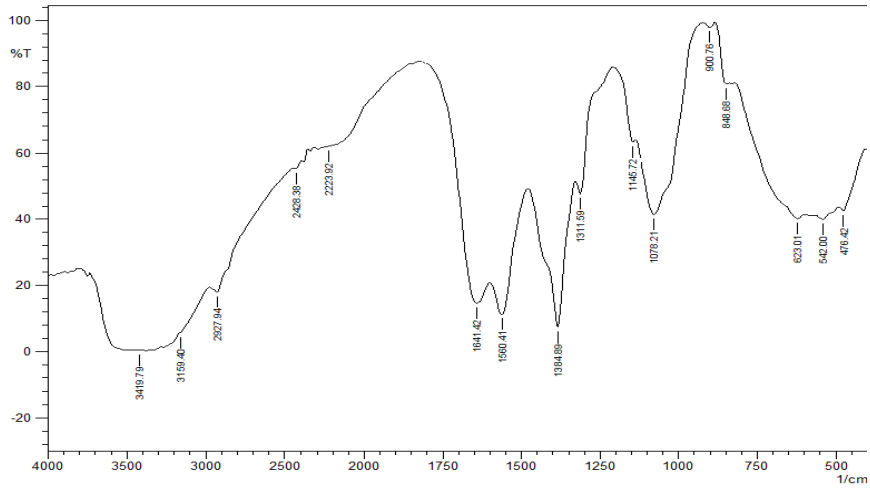

Figure-1 shows the FTIR Spectrum of pure Chitosan oligosaccharide. The spectrum shows absorption bands at 3419cm^{-1} and 2927cm^{-1}which were assigned to O-H and N-H Stretching vibrations and Symmetric CH stretching vibration respectively (Rakkapao, 2011). The absorption bands which were observed at 1641 cm^{-1}, 1560cm^{-1},1384 cm^{-1} and 1145 cm^{-1} shows the presence of C=O stretching, NH_2 bending vibration, Secondary alcoholic group and -C-O-C- in glycosidic linkage. The C-O stretching vibration appeared at 1078 cm^{-1}.

Figure-2 shows the band observed at 2929cm^{-1} and 2870cm^{-1} were assigned to asymmetric and symmetric –CH stretching vibration (Marta, 2014). The spectrum also displays the adsorption peaks at 2942.50cm^{-1}. The C=O amide linkage and C=C (Zang,et al., 2009) alkene stretching vibration appeared at 1647.92 cm^{-1} and 1627.92 cm^{-1} which explains about the reaction between chitosan oligosaccharide and maleic anhydride and showed the unsaturated acid group was added to chitosan oligosaccharide.Certain strong absorption bands obtained at 1647cm^{-1} and 1548 cm^{-1} were attributed to the C=O stretching and NH bending respectively. Absorption bands located at 1386 and 1107 cm^{-1}, belong to C-O stretching and C-O-C is attributed to glycosidic linkage. From the FTIR spectral results it can be concluded that, formation of graft copolymer of chitosan oligosaccharide – g – maleic anhydride. In pure chitosan oligosaccharide there is no unsaturated acid group but when it was grafted with maleic anhydride showed the C=C alkene stretching vibration. Hence the FTIR results proved the formation of COS – g – MAH copolymer.

After mixing the broad band at 3444 cm^{-1} of the –OH stretching was shifted to 3410cm^{-1}, which overlaps the –NH stretching in the same region represented in Figure-3. Lower peak wave number indicates the stronger interactions (Pawlak and Mucha, 2003). The peak for NH bending at 1540 cm^{-1} was shifted to 1520 cm^{-1} during blending. This result indicated that interactions were present between the hydroxyl groups and the amino groups of COS-g-MAH and PVA (Aoi et al.,1998). It also shows a certain degree of miscibility between the polymers.

The strong band observed at around 2920 cm^{-1} may be attributed to the C-H stretching in methyl group. The absorption bands at 1641cm^{-1}(Amide I) and 1560.41 cm^{-1} (Amide II) correspond to Silk fibroin structure (β sheet) (Mariana Agostini, 2010) shown in Figure-4.

When silk is mixed with the blend, the absorption bands of silk was shifted to a higher wavenumber and was gradually merged with amide carbonyl absorption of glucosamine. Therefore, it could be suggested that the fibrion conformation was a β-sheet structure in the composite .During the composite process, the glucosamine amide II adsorption at 1598 cm^{-1} shifted to a lower waven umber at 1567 cm^{-1}; and the glucosamine amide III adsorption at 1243 cm^{-1} disappeared. This suggests that an interaction would have taken place between the polymers during the composite formation.

Scanning Electron Microscopy

Figure - 5: SEM image of pure chitosan oligosaccharide

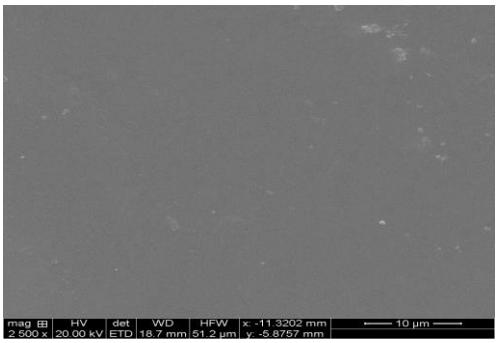

Figure - 6: SEM image of COS–g–MAH

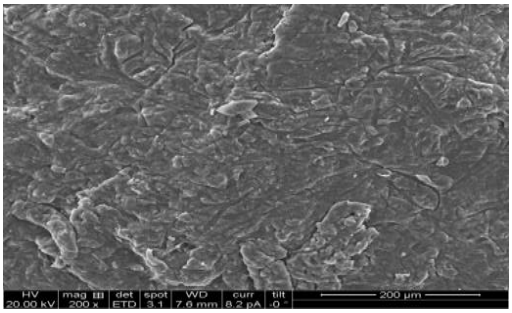

Figure-7 SEM image of COS-g-MAH/PVA /SF (1:1:0.25) composite

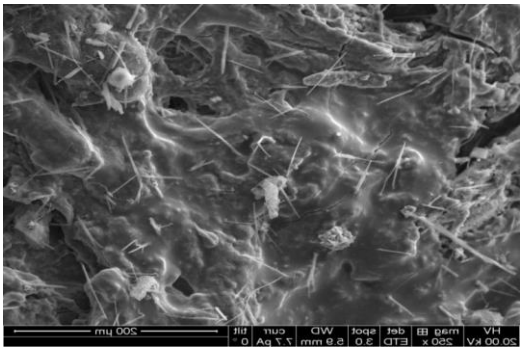

The surface morphology of pure chitosan oligosaccharide was observed by Scanning electron microscope is shown in the Figure - 5. SEM image indicates that the surface of the pure chitosan oligosaccharide was homogenous, uniform, very smooth and regular structure. Hence, the addition of functional groups on the side chains of the pure chitosan oligosaccharide through the grafting process exhibits considerable changes and enhances the material suitable for adsorption process.

Figure-- 6 shows the SEM image of the chitosan oligosaccharide-g-maleic anhydride copolymer. From the image it was observed that the chitosan oligosaccharide-g-maleic anhydride has rough surface when compared with the pure chitosan oligosaccharide. The presence of highly porous surface enhances the adsorption process effectively. This is due to the grafting of maleic anhydride with chitosan oligosaccharide. It is evident from the figure that the grafting has taken place as well.

The above Figure- 7 shows that the SEM image of ternary composite COS-g-MAH/PVA /silk for the ratio (1:1:0.25). The surface morphology of the prepared ternary composite shows that porous, rough and needle like structure which is the main characteristic creteria for the absorbing capacity of the adsorbent. It clearly indicated that there is a small opening in the SEM image which is due to the addition of the silk fibroin material. The porous nature of the ternary blend is due to the addition of the silk fibroin which

increases the rigid structure of the material suitable for absorption process. (1:1:0.25) ratio has higher adsorbing capacity due to the greater rough and porous nature of the blend which was further proceeded for the adsorption process.

Effect of pH

A well characterized important factor is the pH of the aqueous solution which plays a vital role in metal ion adsorption process. Since the pH of the solution controls the surface charge of the adsorbent and the degree of ionization of the adsorbate it has a major impact on the metal uptake amount. The contribution of pH on the metal ion uptake properties of COS-g-MAH/PVA/SF composite toward Pb (II) and Cu(II) ions were studied in pH 3.0-8.0 at room temperature and the results of this study are represented in Figure-8 .

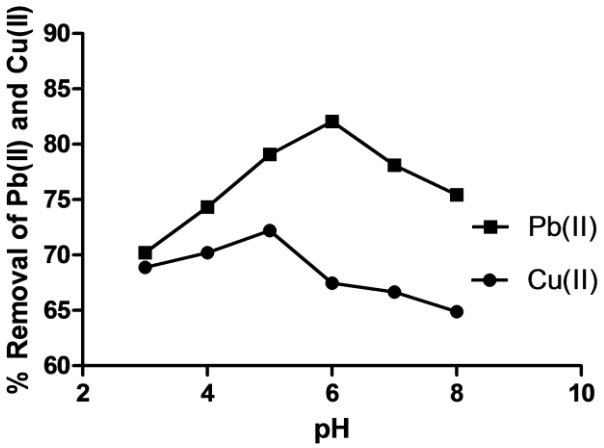

Figure –8: Effect of pH on the removal of (a) copper (II) (b) lead (II) from aqueous solution using COS-g-MAH/PVA/SF composite

From the results presented in Figure- 8 ,it was evident that the percentage of Lead(II) and Copper (II) sorption process were found to gradually increase from pH 3.0 to pH 4.0 followed by a significant increase to a maximum value at pH 6.0 for Lead(II) and thereafter it declines. The maximum percentage removal of Pb (II) value was observed at pH 6 and for Cu(II) at pH 5.

The obtained lesser removal efficiency at low pH was mainly due to the partial protonation of the lone pair of electrons of N and O atoms and a competitive adsorption between H^+ and metal ions which hinders the corresponding COS-g-MAH/PVA/SF composite–metal complex (Fan et al., 2011). The significant increase in Pb (II) and Cu(II) uptake in the range of pH 3.0-6.0, is mainly due to the decreased competition between the H^+ and Pb(II), Cu(II) ions and the decrease in the positive charge of the functional groups (Govindarajan et al., 2011). The lesser uptake of Pb (II) and Cu (II) beyond optimum pH might be due to the deposition of lead as lead hydroxide and copper as copper hydroxide. The formation of these hydroxylated complexes of metal ions would have hindered the metal-binding capacity.

Effect of contact time

The contact time is an effective factor in a batch process. The effect of contact time was evaluated by changing the contact time from 60 mins to 300 mins by keeping all the parameters such as initial concentration of metal ions (200 ppm), adsorbent dose (1g/L), pH (6) as constant. The effect of contact time on the adsorption of Pb(II) and Cu(II) onto COS-g-MAH/PVA/SF composite was investigated using the batch technique and the obtained results are represented in Figure-9 .

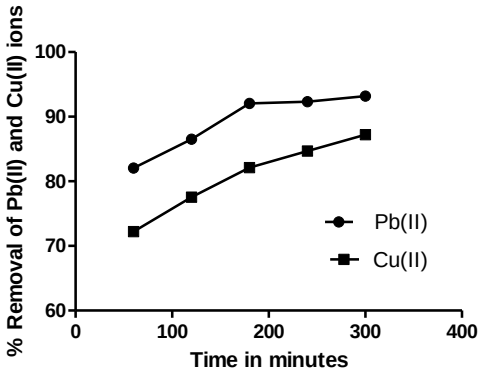

Figure –9: Effect of contact time on the removal of copper (II) and lead (II) from aqueous solution using COS-g-MAH/PVA/SF composite

The result outlined in this study (Figure - 9) concludes that at the initial stage, the adsorption process was however very rapid but as the reaction approached the equilibrium stage, it slowed down. The reason behind the fact is that the sorption processes of Pb (II) and Cu (II) ions by COS-g-MAH/PVA/SF composite sorbent was found to follow two successive steps. The first step involves a rapid increase in the percentage removal of the Pb(II) and Cu(II) ion owing to the abundant availability of active binding sites on surface which permits the rapid accumulation of Pb (II) and Cu(II) ions on the pore sites of the COS-g-MAH/PVA/SF composite (Balarak and Bazrafshan, 2016). The second step is that beyond a certain contact time (180 minutes), due to the complete saturation of the sorbent surface with the metal ions i.e. the active sites occupation, the equilibrium is reached and hence it shows a constant percentage removal (Sivakami et al., 2013).

Contact time is one of the important factors in batch adsorption process. Figure-9 shows a rapid initial adsorption rate of Cu(II) and Pb(II)at the beginning until 180 minutes of contact time, thereafter the adsorption ratebecame practically constant (reached equilibrium) (Ahmaruzzaman and Gayatry, 2010). The initial increase of percentage removal of Cu(II) and Pb(II) fromaqueous solution as a function of contact time was due to the availability of large number of vacant surface sites for adsorption process but after a lapse of timeonly less remaining vacant surface sites were on hand and hence the percentage removal become practically constant.

Effect of adsorbent dose

In order to determine the effect of the biosorbent dosage on the biosorption efficiency of COS-g-MAH/PVA/SF composite, the amount of biosorbent added into the biosorption medium were varied from 1g to 5g by keeping other variables such as initial concentration of lead ions (200 mg/L), contact time: 60mins and pH (6) as constant. Figure-10 represents the effect of adsorbent dose on the adsorption behavior of Pb (II) onto the COS-g-MAH/PVA/SF composite.

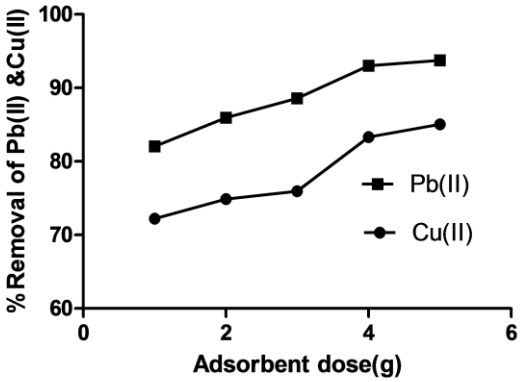

Figure –10: Effect of adsorbent dose on the removal of lead (II) and copper (II) from aqueous solution using COS-g-MAH/PVA/SF composite

The results of this study indicate that upon increasing the adsorbent dosage, it showed an increased percentage removal of Pb (II) and Cu (II). With increase in the biosorbent dosage, from 1g to 5g the percentage removal of Pb (II) and Cu (II) increased from 82.06% to 93.75% for lead and 72.22% to 85.05% for copper. The initial increase in the metal ion removal percentage with increase in adsorbent dosage was due to the greater availability of the exchangeable sites or surface area provided by the adsorbent necessary for the adsorption to occur while increasing the concentration of adsorbent dose (Balarak et al., 2016).

Any further addition of the adsorbent beyond the optimum adsorbent dosage (4g) for both copper (II) and lead (II) ions did not cause that much significant change in the adsorption. Therefore, the optimum adsorbent dosage was found to be 4g for both lead and copper metal ions. Upon increasing the adsorbent mass, the availability of active sites for coordination and binding with the target metal ion was increased and hence it shows an increased percentage removal but beyond optimum adsorbent dosage (4g/100ml), due to the overlapping or aggregation of adsorption sites the total adsorbent surface area available to the metal ions decreased and hence it leads to the equilibrium situation resulting in the constant Pb(II) and Cu(II) percentage removal (Crini et al., 2008).

Effect of initial concentration

The accumulation of metal at the interface between the solid/liquid phases is generally termed as the metal adsorption which is a mass transfer process. The initial metal concentration is an important factor in determining the adsorption potency of a biomass. The influence of metal ion concentration on the adsorption behavior of Pb(II) and Cu(II) ion onto COS-g-MAH/PVA/SF composite was investigated by varying it in the range of 1000, 750, 500, 250 and 125 mg/L, while keeping the other parameters at a constant value. Figure-11 shows the equilibrium adsorption uptake of the sorbent at different initial heavy metal ions concentrations.

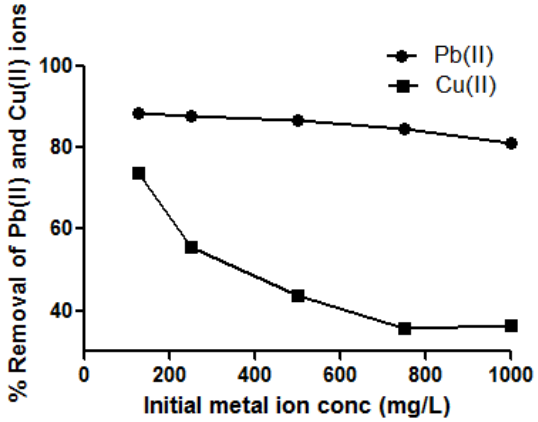

Figure – 11: Effect of initial metal ion conc on the removal of lead (II) and copper (II) from aqueous solution using COS-g-MAH/PVA/SF composite.

The results presented in the Figure-11 reveals that the percent adsorption decreased with increase in initial Lead (II) and Copper (II) ions concentration. At lower concentration, the metal ions would interact with the binding sites and thus facilitated almost 100% adsorption and this can be attributed to availability of vacant sites for metal binding whereas at higher concentrations, the active sites of biosorbents are less available, more ions are left unadsorbed in the solution due to the saturation of the binding sites and hence metal ion removal is reduced The decrease in percentage of adsorption with an increase in initial metal ion concentration might also be due to the increased driving force which develops the concentration gradient between the bulk solution and surface of the COS-g-MAH/PVA/SF composite adsorbent.

The percentage removal of both Pb (II) and Cu(II) has been found to be higher at lower concentration of metal ion solution. A maximum copper removal of 73.96% and lead removal of 88.67% has been obtained for COS-g-MAH/PVA/SF composite. This obtained

result reveals that COS-g-MAH/PVA/SF composite act as very good adsorbents even at low metal ion concentration.

Adsorption Isotherm studies of heavy metal lead and copper using COS-g-MAH/PVA/SF.

Equilibrium adsorption isotherm models were mainly employed to describe the equilibrium distribution of sorbed molecules between the solid and liquid phases and also help in determining the capacity of the adsorbent, affinity of adsorbent and the surface properties. This equilibrium adsorption isotherm is essential to determine the capacity and mechanisms to optimize the design of the sorption system. The thermodynamic equilibrium between the specific amounts of metal ions adsorbed onto the surface of a solid (native or functionalized) and the metal ion concentration remaining in solution was understood by the adsorption isotherms.

Several adsorption isotherm models such as Langmuir, Freundlich, Temkin, Sipps, Dubinin Radushkevich, Toth and Redlich Peterson are available for evaluation of the experimental sorption equilibrium data which have been mainly used to fit the adsorption equilibrium. Among the various adsorption isotherm models, in the present work, the most widely used two models namely Langmuir and Freundlich isotherm were utilized to describe the reaction of Pb(II) and Cu(II) ions with COS-g-MAH/PVA/SF composite surface.

At the optimum conditions of adsorbent dose, contact time, pH and initial metal ion concentration of the adsorption of Lead and Copper were analysed. The values were fitted into Langmuir and Freundlich adsorption isotherm. The Langmuir equation is expressed as follows.

Langmuir sorption isotherm

Langmuir model explains monolayer adsorption on an energetically uniform surface on which there is no interaction between the adsorbed molecules (i.e) once a site was filled, no further sorption can take place at that site. Once monolayer formation was completely saturated then equilibrium was attained.

The Langmuir model is given as follows,

$C_{eq}/C_{ads} = bC_{eq}/K_L + 1/K_L$ --------- (1)

$C_{max} = K_L/b$ ----------(2)

where

C_{ads} = amount of metal ions adsorbed (mg g^{-1})

C_{eq} = equilibrium concentration of metal ion in solution (mg dm^{-3})

K_L = Langmuir constant ($dm^3.g^{-1}$)

b = Langmuir constant ($dm^3.g^{-1}$)

C_{max} = maximum metal ion to adsorb onto 1g adsorbent (mg. g^{-1})

The constant "b" in the Langmuir equation is related to the energy or the net enthalpy of the sorption process. The enthalpy of adsorption can be determined by using constant K_L. The constants "b" and "K_L" are the characteristics of the Langmuir equation and can be determined from the linearized form of the Langmuir equation.

The Langmuir equation was used to explain the data obtained from the adsorption of Pb (II) and Cu(II) ions by graft copolymer composite over the entire concentration range. A plot of C_{eq}/C_{ads} against C_{eq} gives a straight line was shown in Figure-12 and 13 The results of the adsorption isotherm in Table-1 shows a good correlation by the composite. The C_{max} value was 168.93 mg.g^{-1} for lead and for copper it was 23.88mg.g^{-1}. Correlation factor R^2 for lead was 0.9929 and for copper it was 0.9804.

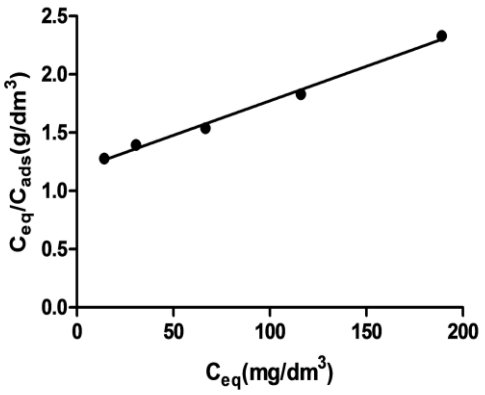

Figure – 12: Langmuir adsorption isotherm plot for Lead (II) onto COS-g-MAH/PVA /SF composite

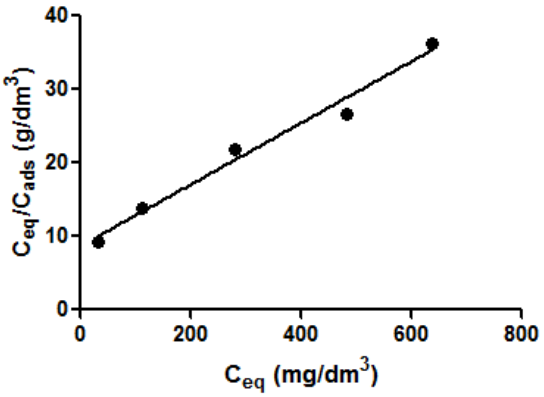

Figure – 13: Langmuir adsorption isotherm plot for Copper (II) onto COS-g-MAH/PVA /SF composite

Table 1: Adsorption isotherm constant, Cmax and correlation coefficients

Metal ions	Langmuir Constants			
	K_L (dm³/g)	b(dm³/mg)	C_{max}(mg/g)	R^2
Pb (II)	0.8460	0.005008	168.93	0.9929
Cu (II)	0.1151	0.004820	23.88	0.9804

R_L the separation factor is used to predict if an adsorption system is "favourable" or "un favourable" (Ngah and Musa, 1998). The separation factor R_L can be calculated using the following expression.

$R_L = 1/1+bC_f$

Where b (L/mg) refers to the Langmuir constant and $C_f$is denoted to the adsorbate final concentration (mg/L). Four different values of R_L, the equilibrium parameter like R_L=1, R_L=0, R_L >1 and 0< R_L<1 was reported by many researchers. These four values symbolize linear adsorption, irreversible adsorption, un-favorable and favorable adsorption process respectively. The calculated values of the separation factor (R_L) were shown in Table- 1

Table- 2: R_L values based on Langmuir adsorption isotherm

Metal ions	Initial Concentration (mg/dm³)	Final concentration (mg/dm³)	R_L Values
	1000	189.1	0.51360
	750	116.1	0.63234
Pb (II)	500	66.65	0.749747
	250	32.5	0.860023
	125	14.175	0.933717
	1000	636.68	0.29002
	750	482.87	0.35036
Cu (II)	500	280.98	0.48102
	250	110.74	0.7016
	125	32.55	0.8899

In the present study since the calculated values of R_L (Table-2) was found to be greater than 0 and less than 1(0<R_L<1), it was concluded that the adsorption of Pb(II) and Cu(II) onto COS-g-MAH/PVA/SF composite was considered to be favorable and the adsorption process would be spontaneous.

A plot of Ce/qevs. Ce yielded a straight line, confirming the applicability of the Langmuir adsorption isotherm. The linearity of the two plots supports the monolayer adsorption and the biosorption depends on the concentration and pH of the metal solutions. Thus, it is found that the adsorption of Pb (II) and Cu (II) onto

chitosan grafted copolymers correlates well with Langmuir equation. For Langmuir isotherm model the homogeneous surface condition of adsorbent is required for monolayer adsorption, which was well described by the values obtained from the plot. Hence the monolayer adsorption was taken place in case of prepared COS-g-MAH/PVA/SF composite.

Freundlich isotherm model

Freundlich model describes the distribution of solute between solid and aqueous phases at the point of saturation. This model mainly assumes heterogeneous surface with a nonuniform distribution of biosorption over the surface and the site energies of biosorbent vary exponentially.

The Freundlich equation is given as

$q_e = K_f C_e^{1/n}$

The linear form of Freundlich equation is expressed as:

$\log q_e = \log K_F + 1/n \log C_e$

A plot of log q_e versus log C_e gives a straight line of slope (1/n) and an intercept of log K_F.

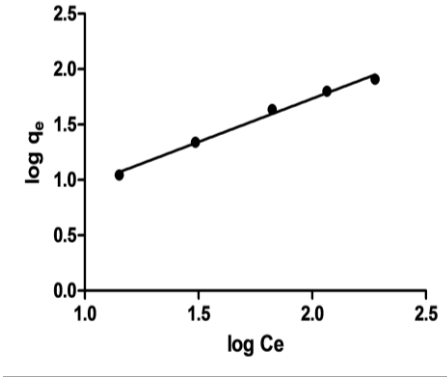

Figure- 14: Freundlich adsorption isotherm plot for lead (II) on to COS-g-MAH/PVA /SF composite

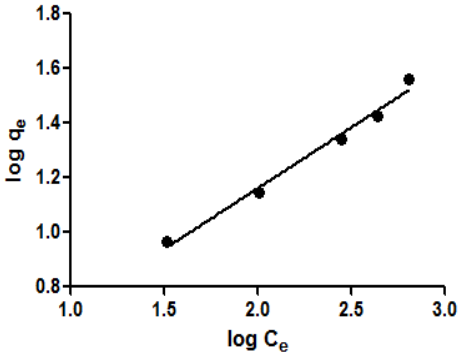

Figure - 15: Freundlich adsorption isotherm plot for copper (II) on to COS-g-MAH/PVA /SF composite.

Table- 3: Freundlich adsorption isotherm constant parameter for lead (II) and copper (II) on to COS-g-MAH/PVA /SF composite.

Metal ions	Freundlich constant		
	K_f	N	R^2
Pb (II)	1.4815	1.2794	0.9912
Cu (II)	1.8801	2.2686	0.9763

The Freundlich constants K_f values were 1.4815 for Pb (II)and 1.8801 for Cu (II) ions and n values were 1.2794and 2.2686 for lead and copper ions respectively. Other than homogeneous surface, the Freundlich equation is also suitable for a highly, heterogeneous surface and an adsorption isotherm shows the formation multilayer adsorption. The value of 1/n is less than unity indicating the significant adsorption at low concentration. The "n" value lies between 1 and 10 which represents beneficial adsorption (Amarasinghe and Williams, 2007).

Table-4 : Comparison between Langmuir and Freundlich constants parameter for lead (II) and copper (II) on to COS-g-MAH/PVA /SF composite

Metal ions	Langmuir constants				Freundlich constant		
	K_L (dm^3/g)	B (dm^3/mg)	C_{max} (mg/g)	R^2	K_f	n	R^2
Pb (II)	0.8460	0.005008	168.93	0.9929	1.4815	1.2794	0.9912
Cu (II)	0.1151	0.004820	23.88	0.9804	1.8801	2.2686	0.9763

Table-3 shows the Langmuir constants and freundlich constants calculated from the slope and intercept of the linear plots. The calculated higher C_{max} values from Langmuir plot suggest that the prepared COS-g-MAH/PVA/SF composite has more potential to remove lead ions from aqueous solution more efficiently than copper ions. In Freundlich adsorption isotherm model, the prediction of 1/n values indicate the type of isotherm to be either irreversible (1/n = 0), favorable (0<1/n<1), unfavorable (1/n>1).

From Table-4, it is evident that the value of n of Freundlich model falling in the range of 1–10 and hence the calculated results suggest that the adsorption of metal ionsonto COS-g- MAH/PVA/SF composite biosorbents was found to behighly favourable suggesting multilayer phenomenon. Based onthe higher R^2values it was concluded that the Langmuir isothermwas the most suitable for the absorption of Pb (II) and Cu (II) onto chitosan oligosaccharide-graft-maleic anhydride/polyvinyl alcohol/silk fibroin composite suggesting that the monolayer chemisorption process takes place effectively.

Kinetics studies

Kinetic investigation was performed to determine the suitable model for the reaction rates and mechanism based on the optimum conditions developed throughout the experiments. In the present work, the controlling mechanisms of biosorption process, chemical reaction, diffusion control and the mass transfer process were examined by utilizing several kinetic models namely pseudo first order, pseudo second order and intraparticle diffusion model.

The kinetics of Copper (II) and Lead (II) biosorption was analyzed using pseudo-first-order and pseudo-second-order (Ho and Mckay, 1999) kinetics models.

The linearized form of first order Lagergren equation is given as Eq. (1).

$$\log (q_e - q_t) = \log q_e - \frac{k_1 t}{2.303} \quad \text{---------} \quad (1)$$

The pseudo-second-order rate equation is given as Eq. (2) (Ho and Mckay, 1999)

$$\frac{t}{q_t} = \frac{1}{k_2 q_e^2} + \frac{t}{q_e} \quad (2)$$

Where, qe and q_t are the amounts of metal adsorbed (mg/g) at equilibrium and at time t (min), k_1 (min^{-1}) and k_2 (g mg^{-1} min^{-1}) are the adsorption rate constant of pseudo-first-order, pseudo-second-order adsorption rate, respectively.

The linear plots of log (q_e - q_t) versus t and (t/q_t) versus t are drawn for the pseudo-first-order and the pseudo-second-order models, respectively. The rate constants k_1 and k_2 can be obtained from the plot of experimental data.

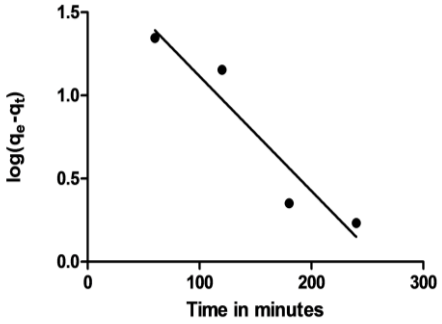

Figure-16: Pseudo first order kinetic plot for Pb (II)

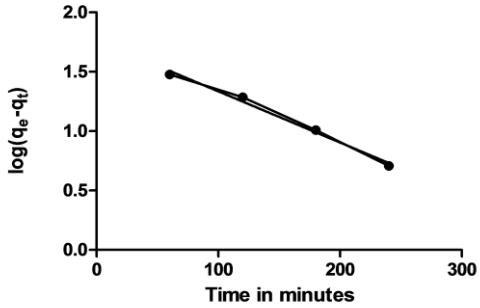

Figure-17: Pseudo first order kinetic plot for Cu (II)

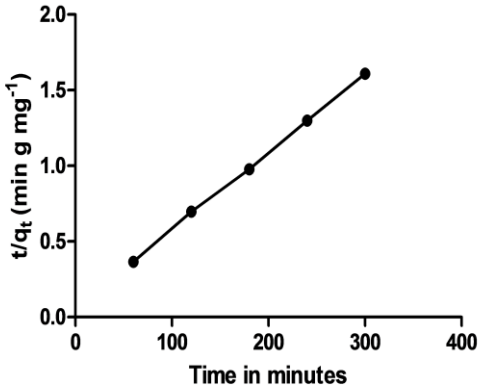

Figure-18: Pseudo second order kinetic plot for Pb(II)

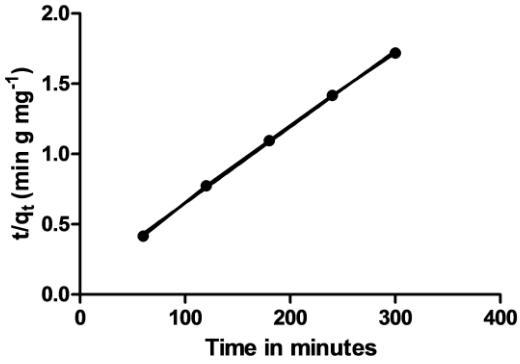

Figure-19: Pseudo second order kinetic plot for Cu (II)

Table-5: Comparison between Lagergren Pseudo-first order and Pseudo-second order kinetics and intraparticle diffusion models for Lead (II) and copper (II) adsorption by COS-g-MAH/PVA /SF composite

Metal	Pseudo-first-order kinetic model			Experimental value	Pseudo-second-order kinetic model		
	qe (mg/g)	k_1 (min^{-1})	R^2	qe (mg/g)	qe (mg/g)	k_2 ($g\ mg^{-1}\ min^{-1}$)	R^2
Pb (II)	63.97	0.01589	0.9099	177.33	194.099	0.000424	0.9995
Cu (II)	58.38	01.2843	0.9904	147.92	185.18	0.000267	0.9991

The results presented in the Figure 16-19 and Table-5 reveals that the linear regression indicates an excellent statistical validity for the pseudo-second order kinetics, as shown by the statistical parameters. The correlation coefficients R^2 obtained for Pb(II) and Cu(II) adsorption onto COS-g-MAH/PVA/SF composite in case of pseudo-second order kinetics were more closer to one and hence from the obtained higher R^2 value it

was evident that the biosorption process followed the pseudo-second-order kinetic model when compared to the pseudo-first-order kinetic model.

In addition to this, the excellent agreement of theoretical loading capacity (q_e) values derived from pseudo second order plots with the experimental values (q_e) calculated from kinetic experiments also agrees with the applicability of pseudo second order kinetic model for COS-g-MAH/PVA/SF composite. The above observations conclude that the adsorption of Lead (II) and Copper (II) ions onto COS-g-MAH/PVA/SF composite follows pseudo second order kinetic model.

FTIR studies

The FTIR spectrum of Chitosan Oligosaccharide /Poly Vinyl Alcohol/ Silk fibroin (1:1:0.25) composites Before and After M(II) adsorption was shown in Figures 20 and 21.

Figure 20: FTIR Spectrum of Chitosan Oligosaccharide /PolyVinyl Alcohol/ Silk fibroin (1:1:0.25) composites After Adsorption of Lead

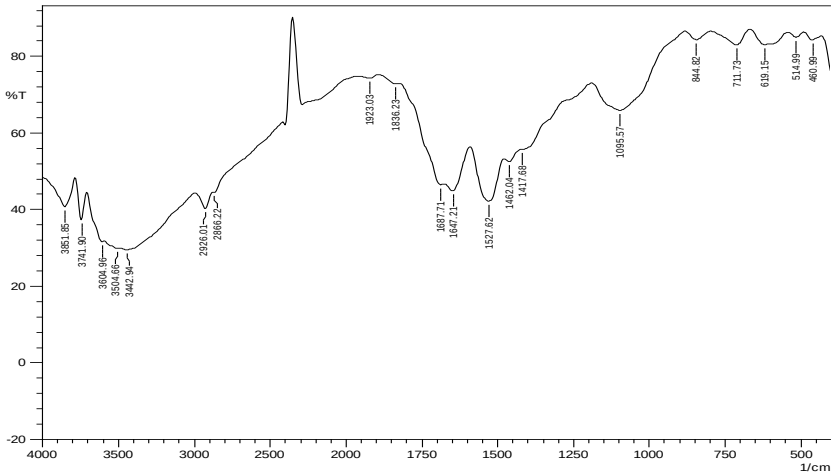

Figure 21: FTIR Spectrum of Chitosan Oligosaccharide /Poly Vinyl Alcohol/ Silk fibroin (1:1:0.25) composites After Adsorption of Copper

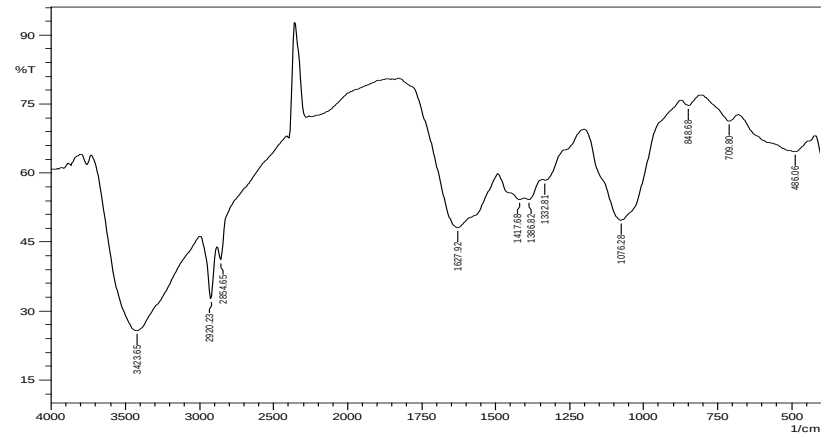

The FT-IR spectral details of chitosan oligosaccharide-graft-maleic anhydride /polyvinyl alcohol/silk fibroin composite (1:1:0.25) ratio after Pb(II) and Cu(II) ion adsorption (Figure 20 and 21) shows a broad peak at 3442 cm^{-1} corresponding to the presence of intermolecular hydrogen bonded OH stretching. On comparing with the FTIR spectrum of chitosan oligosaccharide-graft-maleic anhydride /polyvinyl alcohol/silk fibroin composite before adsorption, after metal adsorption, the shift in the OH band from 3419 to 3442 cm^{-1}after lead adsorption and from 3419 to 3423 cm^{-1} after copper adsorption was observed.

Generally, the metal ions chelate with the carboxylate and hydroxyl groups of macromolecular chains through partially ionic and partially coordinate bonds, respectively (Awad et al., 1980; Awad and Elcheikh,

1981). After the adsorption of metal ions, it was also observed that the stretching vibrations due to the carboxylate ion group (Said and Hassan,1993; Khairou,2002) is shifted to lower wave number (Jin and Bai, 2002; Lin and Bai, 2005a).

The metal - carbon, metal - nitrogen and metal - oxygen stretching frequencies in the spectra of adsorbed species (metal-adsorbate) were observed in the region of around 200-450 cm^{-1} (Niemantsverdri et, 2007). In the case of metal loaded composite the new peaks were appeared at 500 cm^{-1} after metal adsorption due to M-N/ M-O stretching vibrations and this indicate that the nitrogen atom and oxygen atom were found to be the main active sites for metal ion attachment. Hence from the above observations it was concluded that during the metal ion adsorption process the functional groups such as NH_2, OH groups, COO- groups present in the composite were involved in the dative bond formation with the metal.

Figure - 22: EDX image of COS–g–MAH/PVA/SF (1:1:0.25) composite

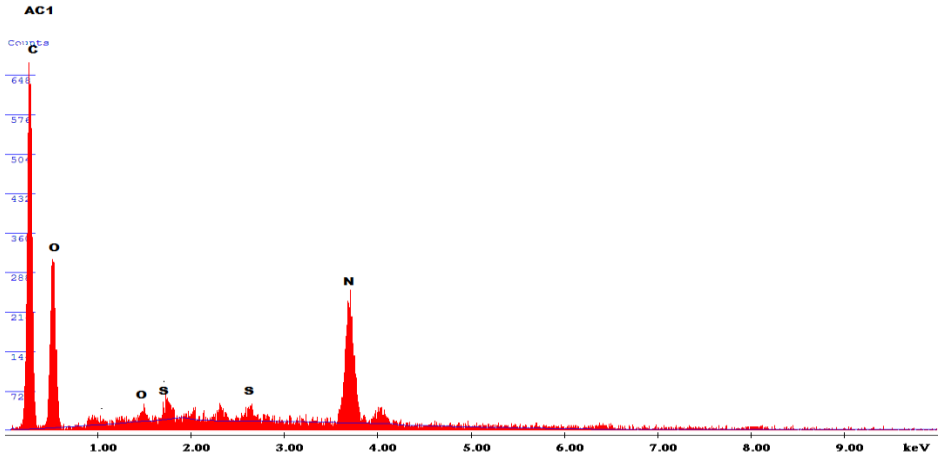

Figure illustrates the EDX image of COS-g-MAH/PVA/SF composite in the ratio (1:1:0.25) which shows the elemental composition of the species present in the composite. Peaks are appearing for Oxygen, Hydrogen and Nitrogen atoms from 1 to 4 keV, showing the composition of the composite.

Figure-22: EDX image of COS–g–MAH/PVA/SF (1:1:0.25) composite - After Pb Adsorption

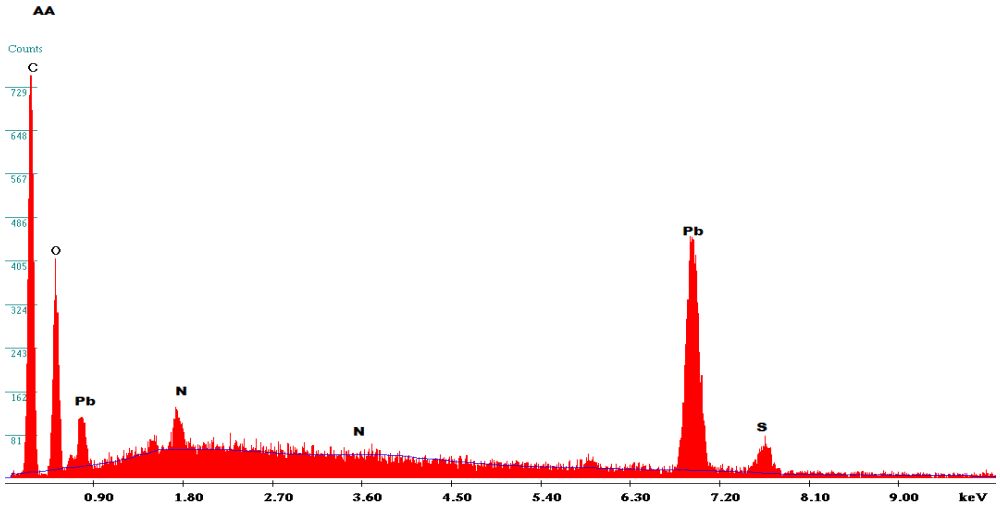

Figure-23: EDX image of COS–g–MAH/PVA/SF (1:1:0.25) composite- After Cu Adsorption

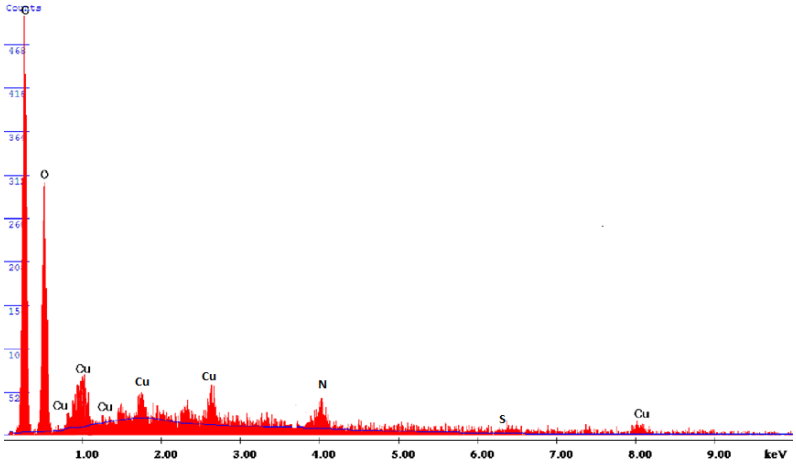

To confirm the presence of Pb^{2+}, Cu^{2+} ions on adsorbed composite EDX spectraof the composites loaded with Pb^{2+}, Cu^{2+}respectively are illustrated in Figure 22 and 23. The EDX spectra showed lead, copper peaks which are indicative of the existence of Pb^{2+}, Cu^{2+}ions on the COS-g-MAH/PVA/Silk fibroin composite showing the effective adsorption of the metals (Ghaee and Shariaty 2012; Yusoff and Kamari 2014).

The higher peaks of lead show the higher adsorption capacity of the composite for the metal lead than copper which is in correlation with the Cmax value of the two metals. (Ghaee et al.,2012). Overall results EDX analysis suggested that the adsorbents studied are capable of binding metal ions. (Zhu et al.,2017)

Based on the above results, the following mechanisms were proposed for the adsorption of metals on the composites. The formation of composites involves both electrostatic and hydrogen bonding and the binding of metal ions onto the composites whereas mostly involve coordination and ion exchange mechanisms.

Removal of lead and copper from the aqueous solution of COS-g-MAH/PVA/SF composites were analyzed by changing pH, contact time, adsorbent dose and initial metal ion concentration. Optimum pH was 6 for Pb (II) and 5 for Cu (II) ions. On increasing adsorbent dose and contact time the adsorption also increased and attained equilibrium at 5g/L and 300 minutes. Monolayer adsorption and second order kinetics were favored on removal of lead and copper.

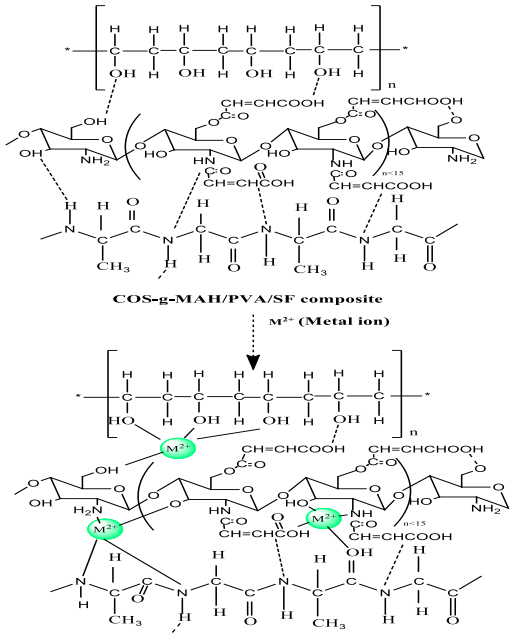

Figure-24: Proposed mechanism for the binding of metal ions on to COS-g-MAH/PVA/SF composite

CONCLUSION

The characteristics of COS-g-MAH/PVA/SF composite were studied using the Fourier transform infrared (FTIR) and (SEM), which confirmed the successful modification process. The results of this research indicated that the novel chitosan oligosaccharide-graft- maleic anhydride/polyvinyl alcohol/silk fibroin (COS-g-MAH/PVA/SF) composite were successfully prepared. The best fitting adsorption model is Langmuir model and the maximum biosorption capacities. Batch adsorption studies was carried out to study the removal efficiency of the prepared composite by varying the parameters such as pH, contact time, adsorbent dose and initial metal ion concentration using the synthetic lead and copper solution. From the results, it was concluded that the graft copolymer was found to be an efficient adsorbent.

REFERENCES

Yasmin Regina, M., Saraswathy S., Kamal, B., Karthik, V. and. Muthukumaran, K. (2015). Removal of nickel (ii) ions from waste water using low cost adsorbents: A review. J. Chem. Pharm. Sci. 8:1-6.

Chehregani, A.B. Malayeri, G. and Golmohammadi, R. (2004). Effect of heavy metals on the developmental stages of ovules and embryonic sac in Euphorbia cheirandenia. Pakistan Journal of Biological Sciences. 8:622-625

Mano, J.F., Sousa, R.A., Boesel, L.F., Neves, N.M., Reis, R.L. (2004). Bioinert, biodegradable and bioinjectable polymeric matrix composites for hard tissue replacement: state of the art and recent developments. Composites Science and Technology. 64:789-817.

Zhang, B., Wang, D., Li, H., Xu, Y. and Zhang, L. (2009). Preparation and properties of chitosan–soybean trypsin inhibitor blend film with anti- Aspergillus flavus activity. Ind. Crops. Prod.29(2-3):541–548.

Dong, Y. and Feng, S.S. (2006).Nanoparticles of poly (D, L-lactide)/methoxy poly (ethylene glycol)-poly (D, L-lactide) blends for controlled release of paclitaxel. Journal of Biomedical Materials Research Part A.78 (1):12-19.

Vijay Kumar Thakur, Manju Kumari Thakur (eds.) (2015). Eco-friendly Polymer Nanocomposites: Chemistry and Applications. Advanced Structure materials Series.74: 122-145.

Karen Deleersnyder, Stijn Schaltin, Jan Fransaer, Koen Binnemans and Tatjana N. Parac Vogt (2009). Ceric ammonium nitrate (CAN) as oxidizing or nitrating reagent for organic reactions in ionic liquids. Tetrahedron Letters. 50:4582–4586.

Mirabedini, S. M., Rahimi, H., Hamedifar, Sh. and Mohseni, S. M. (2004). Microwave irradiation of polypropylene surface: a study on wettability and adhesion. International Journal of Adhesion and Adhesives. 24:163-170.

Farrokh Sharifi, Zhenhua Bai, Reza Montazami and Nastaran Hashemi, (2016), Mechanical and physical properties of poly (vinyl alcohol) microfibers fabricated by a microfluidic approach. RSC Adv.6:55343-55353.

Mohammad Al-Hwaiti, A. Khalid, Ibrahim, Muhanned Harrara (2015). Removal of heavy metals from waste phosphogypsum materials using polyethylene glycol and polyvinyl alcohol polymers, Arabian Journal of Chemistry (2015).

http://dx.doi.org/10.1016/j.arabjc.2015.08.006.

Gopal Reddi, M.R., Gomathi, T., Saranya, M. and Sudha PN (2017). Adsorption and kinetic studies on the removal of chromium and copper onto Chitosan-g-maliec anhydride-g-ethylene di-methacrylate. Int J Biol Macromol.104(Pt B):1578-1585.

Lavanya, R., Gomathi, T., Vijayalakshmi, K., Saranya, M., Sudha, P.N. and Anil, S. (2017). Adsorptive removal of copper (II) and lead (II) using chitosan-g-maleic anhydride-g-methacrylic acid copolymer. Int J Biol Macromol.104(Pt B):1495-1508.

Minoura, N., Tsukada, M. and Nagura, M. (1990). Physico-chemical properties of silk fibroin membrane as a biomaterial. Biomaterials. 11:430-434.

L.Xu, Y.A.,Huang, Q.J.Zhu, C.Ye. (2015). Chitosan in molecularly imprinted

Polymers: correct and future prospects, Int.J. Mol.Sci. 16: 18328-18347.

Rakkapao, N., Vao-soongnern, Y. Masubuchi and Watanabe, H.

(2011). Miscibility of chitosan/poly (ethylene oxide) blends and effect of

doping alkali and alkali earth metal ions on chitosan/PEO interaction.

Polymer. 52:2618-2627.

Zhang, B., Wang, D., Li, H., Xu, Y. and Zhang, L. (2009). Preparation

and properties of chitosan–soybean trypsin inhibitor blend film with anti-

Aspergillus flavus activity. Ind. Crops. Prod.29(2-3):541–548.

Pawalak, A. and Mucha, M. (2003). "Thermogravimetric and FTIR

studies of chitosan blends". Thermochimica Acta, 96:153-166.

Mariana Agostini de Moraes., Grinia Michelle Nogueira, Raquel Farias weska and Marisa Masumi Beppu, (2010). Preparation and Characterization of

Insoluble Silk Fibroin/Chitosan Blend Films, polymers.2:719-727.

Govindarajan, C., Ramasubramaniam, S., Gomathi,T. and Sudha, P.N. (2011). Studies on adsorption behavior of Cadmium onto nano chitosan carboxymethyl cellulose blend. Arch. Appl. Sci. Res. 3:572–580.

Balarak, D., Mahdavi, Y., Bazrafshan, E.Mahvi, A.H. and Esfandyari, Y. (2016). Adsorption of fluoride from aqueous solutions by carbon nanotubes: determination of equilibrium, kinetic and thermodynamic parameters. Fluoride.49:71–83.

Sivakami,M. S., Gomathi,T., Venkatesan,J., Jeong,H.S., Kim, S.K. and Sudha, P. (2013). Preparation and characterization of nano chitosan for treatment wastewaters. Int. J. Biol. Macro mol. 57: 204–212.

Ahmaruzzaman, M. and Laxmi Gayatri, S. (2010). Activated tea waste as a low-cost adsorbent for the removal of p- nitrophenol from wastewater. Journal of chemical and engineering and data 55(11):4616-4623.

Crini, F., Gimbert, C., Robert, B., Martel, O., Adam, N., Morin-Crini, et al. (2008). Theremoval of Basic Blue 3 from aqueous solutions by chitosan-based adsorbent: batch studies.J. Hazard. Mater. 153:96–106.

Amarasinghe, B.M.W.P.K. and Williams, R.A. (2007). Tea waste as a low-cost adsorbent for the removal of Cu and Pb from wastewater. Chem. Eng. J. 132: 299–309.

Ho, Y.S. and McKay, G. A. (1998). Comparison of chemisorption kinetic models applied to pollutant removal on various sorbents. Process Safety Environ Protect. 76:332–340.